THE LANCET
Neurology

Supplementary appendix 1

This appendix formed part of the original submission and has been peer reviewed. We post it as supplied by the authors.

Supplement to: Gustavsson EK, Follett J, Trinh J, et al. *RAB32* Ser71Arg in autosomal dominant Parkinson's disease: linkage, association, and functional analyses. *Lancet Neurol* 2024; published online April 10. https://doi.org/10.1016/S1474-4422(24)00121-2.

APPENDIX 1

Table of Contents

SUPPLEMENTARY METHODS

Study sites and ethics protocols

All probands and case-control series for linkage and association analyses were ascertained under ethically approved protocols by each collaborating site between 2001-2018. All DNA was extracted from blood using standard methods, and genotyped for this study at the University of British Columbia, and with appropriate REB approvals (H10-02191, H10-01461 and H11-02030; PI Dr. Matt Farrer). All exome sequencing and analysis was also performed by the Centre for Applied Neurogenetics at the University of British Columbia. Additional clinicogenetic analyses were performed at the University of Florida (IRB#202000632; #202001661; PI Dr. Matt Farrer). All participants were over the age of 18 years.

Whole exome sequencing (WES), variant selection and genotyping

Eligibility for the inclusion of probands was the presence of two or more family members with a diagnosis of PD from whom blood or DNA samples were available. All diagnoses, affected and asymptomatic, were made after a physical exam by a specialty-trained movement disorders neurologist, consistent with UK Brain Bank Criteria (as stated in Methods).

Exonic regions were enriched using the Ion AmpliSeq exome kit (57·7Mb) and sequenced on the Ion Proton (Life Technologies, Carlsbad, CA, USA) with a minimum average coverage of 70 reads per base and an average read length of 150 bases. Reads were mapped to the NCBI Build 37·1 (hg19) reference genome using the Ion Torrent Suite 5·0. Sequences with a mapping Phred quality score under 20, fewer than 10 reads or over 95% strand bias were excluded from further analysis. Variants were annotated with ANNOVAR[2] and Combined Annotation Dependent Depletion (CADD) C-scores[3] to help rank functional, deleterious and disease causal variants.

All known Mendelian genes for parkinsonism published up until 12/2018 were examined and excluded on the basis of exome data and Illumina MEGA array genotyping, as previous. [4–13] The former included genomic loci (all exons) for *ATP6AP2, ATP13AP2, C9orf72, CHCHD2, CSF1R, DCTN1, DJ-1, DNAJC6, DNAJC12, DNAJC13, EIF4G1, FUS, FMR1, GBA, GCH1, GRN, HTT, MAPT, LRRK2, Parkin, PINK1, SCA2, SCA3, SCA6, SCA8, SNCA, SNCB, SYNJ2* and *VPS35*. The latter included copy number analysis of intensity files for *SNCA*, *Parkin* and *PINK1*. Comprehensive gene screening and exclusion has been completed in all affected probands, but not in other family members.

RAB variants were selected for subsequent analysis if they were: (1) good quality calls, greater than 10 reads deep with balanced forward and reverse reads; (2) predicted to be SNVs or insertions/deletions (indels) in an exonic or splicing region; (3) had a minor allele frequency (MAF) of ≤ 0·01 from the genome Aggregation Database (gnomAD v2.1; http://gnomad.broadinstitute.org/), and; (4) were absent in our in-house control exomes (n=312). Subsequent genotyping was performed by Sanger sequencing of specific exons, as previously described or using TaqMan probes (Life Technologies), following the manufacturer's instructions. Positive and negative controls were included to ensure the reliability of all genotyping.

Inclusion in a case-control series was similar; cases with PD were biased to those wishing to participate, potentially with young onset disease and/or a family history of parkinsonism or neurodegeneration, although additional affected family members were not available. Control participants were unrelated, albeit often spouses and/or knowledgeable about PD, and were confirmed to have no family history of parkinsonism or neurodegeneration. Control participants were interviewed and confirmed to be asymptomatic by a neurologist or by a clinical study coordinator trained in movement disorders, prior to inclusion. All were neurologically healthy at the time of their participation.

The majority of case-control samples have been screened and were 'negative' for most frequently observed Mendelian variability in PD, including variants in the *SNCA* locus, *LRRK2 Gly2019Ser*, *DNAJC13 Asn855Ser*, *GBA Asn370Ser & Lys444Pro*, *MAPT* locus and *VPS35 Asp620Asn*. [4–13] All genotyping was performed specifically for this study, including all RAB variants, at the Centre for Applied Neurogenetics between 2066-

2019. Three methods were employed, namely direct Sanger sequencing, specific Taqman probes (assays-by-design) and Agena MASSarray genotyping, as previously described.

Database resources were last accessed between 9-12/2023.

Pathologic diagnoses

The brain was removed within 24 hours of death, with one hemisphere frozen at 80 °C, the other fixed in formalin, and regions embedded in paraffin for dissection and histologic studies to provide a pathologic diagnosis of parkinsonism, as previously described[1].

Haplotype analysis

Single nucleotide polymorphisms (SNP) were genotyped in the Tunisian families (TUN I and TUN2) using Affymetrix 500K *Nsp*I and *Sty*I ships, and genotypes were extracted from .cel intensity files using three algorithms, BBRML, JAPL and CHIAMO, and only included when there was consensus, as previously described.[13] One patient was genotyped on the HumanCyto-12_300K chip (FRA1). Otherwise, Illumina Multi-Ethnic Genome Arrays (MEGA) were used in all other familial probands and the French-Canadian family (CAN I) (**Figure 2**); GenomeStudio® was used to provide genotypes for Illumina data, as previous.[14] DNA from all available family members and samples identified with the putatively pathogenic RAB variant were genotyped, as specified above. Alternatively, genotypes for the same SNPs were retrieved from whole genome data using bcftools. Phase was established within pedigrees when possible.

Structural modelling

AlphaFold modelling[15] was used to predict the interaction between LRRK2 and RAB32. A local installation of ColabFold[16] using MMseqs2 sequence alignment and AlphaFold2-multimer-v3 model, with additional AMBER structure relaxation was employed to model interactions between the LRRK2 fragments (1-1000 or 350-550, Uniprot: Q5S007) and RAB32 (Ser71 WT and Arg71 mutant, Uniprot: Q13637). Resulting structures were visualized and analyzed using PyMOL 2·5·5. BIOVIA Discovery Studio Visualizer 2021 was used to determine possible intermolecular interactions (Non-bond Interaction Monitor) and to predict potential rotamers.

RAB32 mRNA and protein expression across tissues

For *RAB32* mRNA expression we used RNA-seq data for 17,510 human samples originating from 54 different human tissues (GTEx, v8) that were downloaded using the R package recount (v 1·4·6)[17]. Cell lines, sex-specific tissues, and tissues with 10 samples or below were removed. Samples with large chromosomal deletions and duplications or large copy number variation previously associated with disease were filtered out. For RAB32 protein expression we downloaded normal tissue data from Human Protein Atlas https://www.proteinatlas.org/, accessed on 02/08/2023). In addition, we performed immunohistochemical staining in C57BL/6 mice to assess RAB32 expression in TH-expressing cells of the SNpc. Immunohistochemistry was performed, as previously described[18], using primary rabbit anti-mouse RAB32 (ABC520, Millipore; 1:500) and chicken anti-Tyrosine Hydroxylase (ab76442, Abcam; 1:1000). Secondary antibodies used were Alexa Fluor® Goat anti-rabbit, chicken or mouse IgG (H+L) 488 and 568 secondary (1:1000).

Cell culture and constructs

HEK293FT cells were maintained in Dulbecco's Modified Eagle Medium (DMEM, Gibco) supplemented with 10% Heat Inactivated Fetal Bovine Serum (ThermoHEK293 cells (RRID: CVCL_0045) were purchased from the American Type Culture Collection and maintained in DMEM containing 10% (v/v) FBS, 2 mM l-glutamine, penicillin (100 U/ml), and streptomycin (100 μg/ml). All cells were grown at 37°C temperature with 5% CO_2 in a humidified atmosphere and regularly tested for mycoplasma contamination. The following plasmids were used for cell transfection and kinase activity assays: HA-empty vector (DU49303); HA-RAB32 Ser71 wild-type (DU52622); HA-RAB32 Arg71 (DU77801); HA-RAB32 Ala71 (DU77802); HA-RAB29 wild-type (DU50222); Flag-LRRK2 wild-type (DU62804). These were generated by the MRC PPU Reagents and Services at the University of Dundee (https://mrcppureagents.dundee.ac.uk). Each construct was confirmed by sequencing at the

MRC Sequencing and Services (https://www.dnaseq.co.uk). All plasmids are available to request via the MRC PPU Reagents and Services website (https://mrcppureagents.dundee.ac.uk). A detailed description of cell transfection and cell lysis methods have previously been described.[19] Briefly, HEK293 cells were seeded into 6-well plates and transiently transfected at 60-70% confluence using Polyethylenimine (PEI) transfection reagent (Polysciences, Inc., #24765). For each well, 1·6 µg of N-ter Flag-tagged LRRK2 (wild-type or mutant), 0·4 µg of N-ter HA-tagged RAB32 or RAB29 (wild-type, mutant or control) (or HA-empty vector) and 6 µg of PEI were diluted in 0·5 mL of Opti-MEM™ Reduced serum medium (Gibco™) and incubated for 15-20 minutes at room temperature before being added to the cells. Cells were lysed 24 hrs post-transfection in ice-cold lysis buffer containing 50 mM Tris-HCl pH 7·4, 1 mM EGTA, 10 mM 2-glycerophosphate, 50 mM sodium fluoride, 5 mM sodium pyrophosphate, 270 mM sucrose, supplemented with 1 µg/ml microcystin-LR, 1 mM sodium orthovanadate, complete EDTA-free protease inhibitor cocktail (Roche), and 1% (v/v) Triton X-100. Lysates were clarified by centrifugation at 17,000 g at 4 °C for 10 min and supernatants were quantified by Bradford assay.

Quantitative immunoblot analysis

A detailed description of the quantitative immunoblotting protocol has previously been described.[20–22] Briefly, cell lysates were mixed with a quarter of a volume of 4 x SDS-PAGE loading buffer (Invitrogen™ NuPAGE™ LDS Sample Buffer, cat# NP0007) and heated at 70 °C for 5 min. Samples were loaded onto NuPAGE 4–12% Bis–Tris Midi Gels (Thermo Fisher Scientific, Cat# WG1402BOX or Cat# WG1403BOX) and electrophoresed at 130 V for 2 hrs in NuPAGE MOPS SDS running buffer (Thermo Fisher Scientific, Cat# NP0001-02). Proteins were then electrophoretically transferred onto a nitrocellulose membrane (GE Healthcare, Amersham Protran Supported 0·45 µm NC) at 90 V for 100 min on ice in transfer buffer (48 mM Tris base and 39 mM glycine supplemented with 20% (v/v) methanol). The membranes were blocked with 5% (w/v) skim milk powder dissolved in TBS-T (50 mM Tris base, 150 mM sodium chloride (NaCl), 0·1% (v/v) Tween 20) at room temperature for 1 hr before overnight incubation at 4 °C in primary antibodies. Membranes were washed three times for 15 min each with TBS-T before being incubated with secondary antibodies for 1 hr at room temperature. Thereafter, membranes were washed with TBS-T three times with a 15-minute incubation for each wash, and protein bands were acquired via near-infrared fluorescent detection using the LI-COR Odyssey CLx Western Blot imaging system, and intensities of bands were quantified using Image Studio Lite (version 5·2·5, RRID:SCR_013715).

Antibodies used for quantitative immunoblotting analysis

The antibodies against Rab10 Thr73 [MJF-R21] (ab230261) and LRRK2 Ser1292 [MJFR-19-7-8] (ab203181) and the anti-HA tag antibody (ab18181) were purchased from Abcam. The rabbit monoclonal antibody against LRRK2 Ser935 (UDD2) was purified by MRC PPU Reagents and Services at the University of Dundee (https://mrcppureagents.dundee.ac.uk). The mouse monoclonal antibody against total LRRK2 (C-terminus) was purchased from NeuroMab (clone N241A/34, #75-253). The mouse monoclonal against total Rab10 was purchased from Nanotools (#0680–100/Rab10-605B11). All primary antibodies were diluted in 5% (w/v) bovine serum albumin (BSA) in TBS-T and used at a final concentration of 1 µg/ml. Goat anti-mouse IRDye 680LT (#926-68020) and goat anti-rabbit IRDye 800CW (#926-32211) secondary antibodies were from LI-COR and were diluted 1:20,000 (v/v) in 5% (w/v) milk in TBS-T.

Immunocytochemistry and co-localization

For co-transfection of GFP-RAB32, HA-PINK1 and mCherry-Parkin, HEK293 cells were seeded on glass coverslips (Poly-D-Lysine coated) at a density of ~50,000 cells/well in 24-well plates in DMEM media without antibiotics supplemented with 10% FBS (heat inactivated). After 24 hours, cells were co-transfected using lipofectamine 3000 with plasmid constructs as follows: (a). GFP-RAB32 WT (0·5 µg) and HA-PINK1 WT (1·0 µg) and mCherry-Parkin (1·0 µg); (b). GFP-RAB32 WT (0·5 µg) and HA-PINK1 kinase dead (KD) (1·0 µg) and mCherry-Parkin (1·0 µg); (c) GFP-Rab32 Ser71Arg (0·5 µg) and HA-PINK1 WT (1·0 µg) and mCherry-Parkin (1·0 µg); and (d) GFP-Rab32 Ser71Arg (0·5 µg) and HA-PINK1 KD (1·0 µg) and mCherry-Parkin (1·0 µg). 24

hours post-transfection, cells were washed in 1x phosphate buffered solution (PBS) (pH 7·4) and fixed in 10% Formalin (buffered saline, pH 7·4) for 20 minutes at room temperature and permeabilized in 0·1% triton X-100 in 1x PBS for 15 minutes at room temperature with gentle shaking followed by blocking in 10% normal donkey serum in 1x PBS for 1 hour. Cells were incubated with primary mouse mAb anti-HA tag (Thermo-scientific Pierce: PI26183) antibody (1:8000) overnight at 4°C. Cells were washed 3 times for 5 minutes each wash in 1x PBS. Secondary donkey anti-mouse Alexa Fluor 647 antibody (1:1000) was added to the cells and incubated for 2 hours at room temperature with gentle shaking. Primary and secondary antibodies were diluted in 0·02% triton X-100, 1% normal donkey serum in 1x PBS. Cells were washed 3 times for 5 minutes each wash in 1x PBS and mounted using Prolong Diamond anti-fade media (Life Technologies) and allowed to dry overnight before processing for confocal imaging. To assess co-localization between RAB32 and PINK1, a Leica TCS SP5 laser scanning confocal microscope (Leica Microsystem) was used. High resolution images were acquired using 63x oil-immersion (scan averaged, four times; 1024 × 1024 pixel resolution). Initial settings for pinhole, digital gain and noise reduction were optimized and all acquisition parameters were kept the same throughout the imaging. Co-localization was analyzed by Pearson's correlation co-efficient (ImageJ plug-in JACoP). 12-15 cells with comparable co-transfection efficiency were selected for co-localization analysis. Statistical analysis was performed using two-way ANOVA (Graph pad Prism 8·1·1) and presented as mean ± SEM ($p \geq 0{\cdot}0001$).

Image processing and Analysis

Transfected cells were imaged under oil-immersion at 60x magnification on an Olympus FV-1000 confocal laser scanning microscope (9 x 0·33µm step size). Images were stacked using ImageJ software (NIH, USA), and masks were created to encompass the entirety of a cell, excluding the nucleus as labelled by DAPI. Masks and non-manipulated images were processed using a custom pipeline with Cell Profiler software (v·2·1·1) to identify number and density of GFP-RAB32 (-Ser71Arg)-positive structures between 1-3µm in diameter.

SUPPLEMENTARY RESULTS

RAB32 co-localizes with PINK1 but not Parkin.

Phosphoproteomic screens revealed that PD-linked PINK1 mutations alter phosphorylation of several RABs[23,24]. Hence, we examined potential interactions between RAB32 and PINK1. Confocal microscopy of HEK293 cells transiently co-transfected with mCherry-Parkin, GFP-RAB32, and HA-PINK1 revealed significant co-localization of GFP-RAB32 with HA-PINK1 but not with mCherry-Parkin (**Supplementary fig. 9**). Co-localization with PINK1 was significantly reduced in cells transfected with RAB32 Arg71 compared to Ser71, and was reduced to a similar extent as kinase dead PINK1 (KD-PINK1) (**Supplementary fig. 9**). Cells transfected with both RAB32 Arg71 and KD-PINK1 showed the lowest co-localization (**Supplementary fig. 9**). Our results suggest that both PINK1 kinase activity and RAB32 Ser71 are important for PINK1-RAB32 co-localization.

SUPPLEMENTARY FIGURES

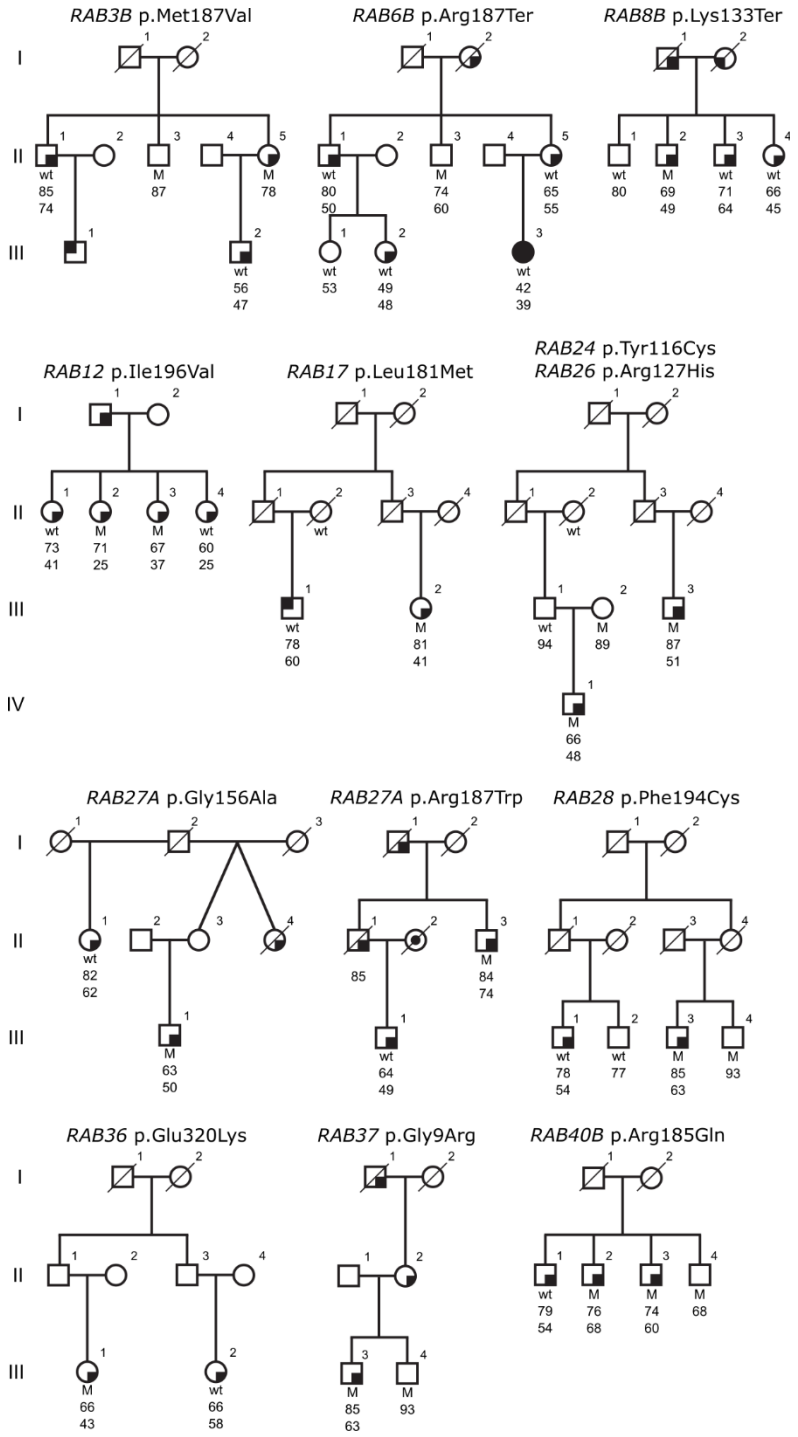

Supplementary Figure 1. Pedigrees with multi-incident parkinsonism. Individual pedigrees are labeled by the variant identified in the proband. 'M' denotes a carrier of the specific variant, and wt stands for wild type. Age (top) and, when available, age at onset (bottom) is denoted under genotype. All pedigrees have affected individuals with M and wt, with the exception of *RAB37* Gly9Arg. This was detected in a 52-year-old male and his 85-year-old mother, both of whom initially presented with resting tremor and were subsequently clinically diagnosed with PD at ages 44 and 61, respectively. The variant was not present in the unaffected father (age unknown) or sister (age 56). This Canadian family of Chinese heritage has a documented family history of the

disease for three generations prior, but no additional clinical information is available. However, *RAB37* Gly9Arg was not found in any additional proband/pedigree, and only 2/130 originated from East Asia. Only one heterozygote is reported in gnomAD (1/628,774 total alleles) and is of European descent.

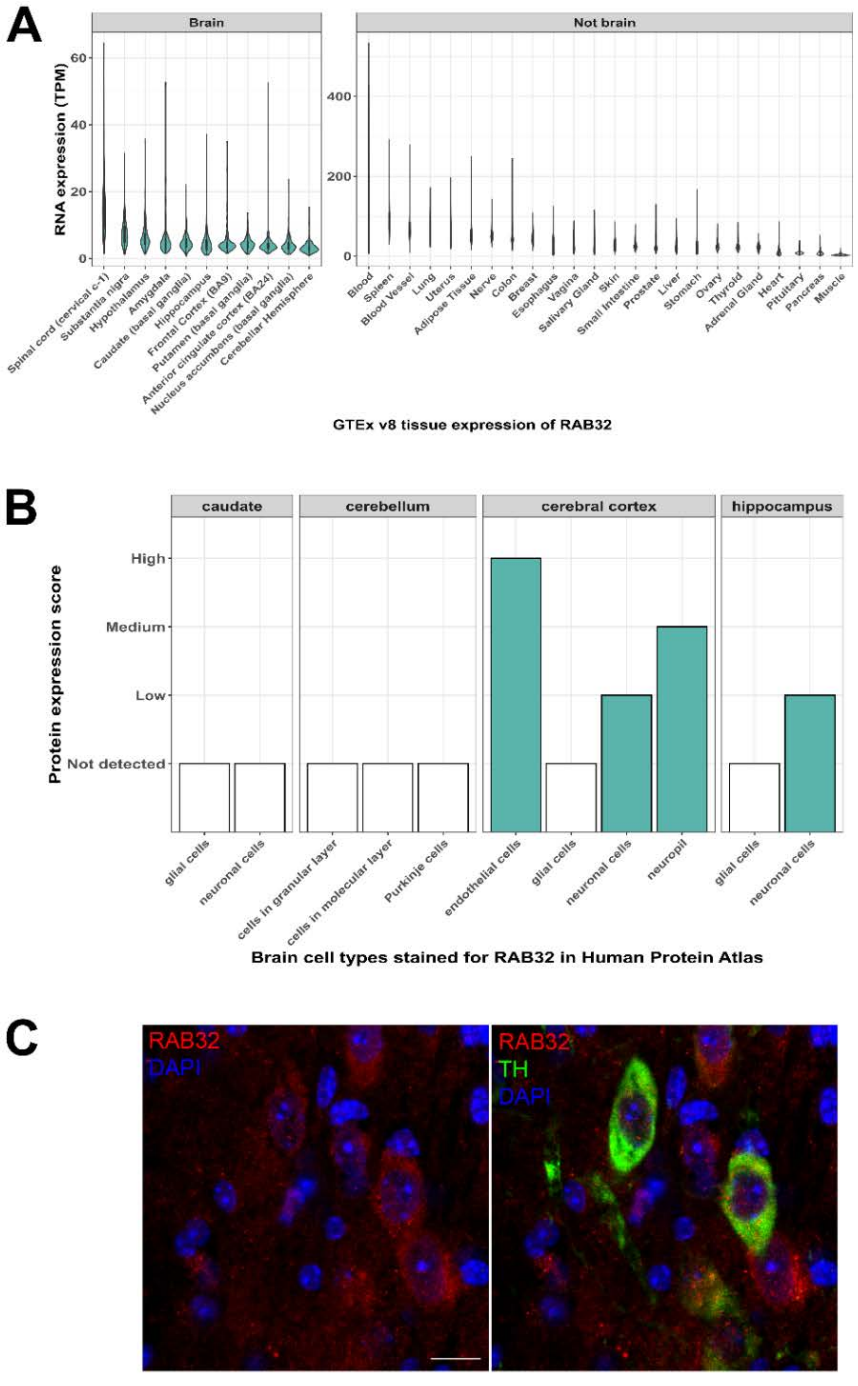

Supplementary Figure 2. A) Transcripts per million (TPM) expression of RAB32 across human tissues generated by the Genotype-Tissue Expression Consortium, GTEx v8). **B)** RAB32 protein expression in brain tissues through Immunohistochemical staining. Data generated by Human Protein Atlas. **C)** Immunohistochemical staining in 3 month old C57BL/6J male mice revealed that RAB32 is expressed in TH-expressing neurons of the *substantia nigra pars compacta*. Animal work was performed under ethically-approved protocols for mouse breeding, brain harvest and immunohistochemistry at the University of British Columbia (PI Dr. Matt Farrer, namely 'A16-0088 - PD breeding protocol v3 and A15-0105- Neurodegenerative Diseases: Physiological and Biochemical procedures).

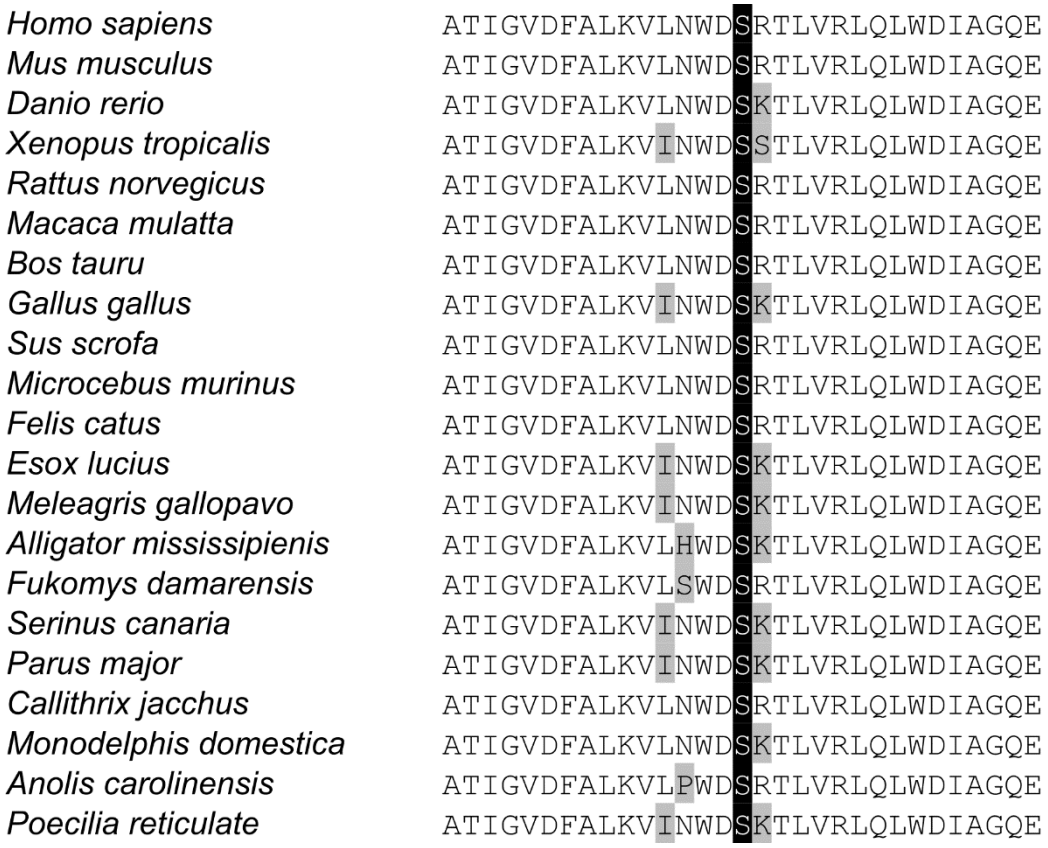

Supplementary Figure 3. Conservation of RAB32 Ser71. Protein homologs were aligned via ClustalO. Amino acid position for RAB32 Ser71Arg (S71R) is highlighted in black. Protein homologs with amino acid positions differing from those of the human RAB32 sequence are indicated in gray. RefSeq accession numbers: *Homo sapiens* (NP_006825), *Mus musculus* (NP_080681), *Danio rerio* (NP_958489), *Xenopus tropicalis* (NP_001011276), *Rattus norvegicus* (NP_001102372), *Macaca mulatta* (NP_001180823), *Bos taurus* (NP_001192879), *Gallus gallus* (NP_001264601), *Sus scrofa* (NP_001116648), *Microcebus murinus* (XP_012607651), *Felis catus* (XP_003986676), *Esox lucius* (XP_010901778), *Meleagris gallopavo* (XP_003204151), *Alligator mississippiensis* (XP_006271694), *Fukomys damarensis* (XP_010624980), *Serinus canaria* (XP_009091018), *Parus major* (XP_015478707), *Callithrix jacchus* (XP_002747112), *Monodelphis domestica* (XP_001370750), *Anolis carolinensis* (XP_003215798) and *Poecilia reticulata* (XP_008395960).

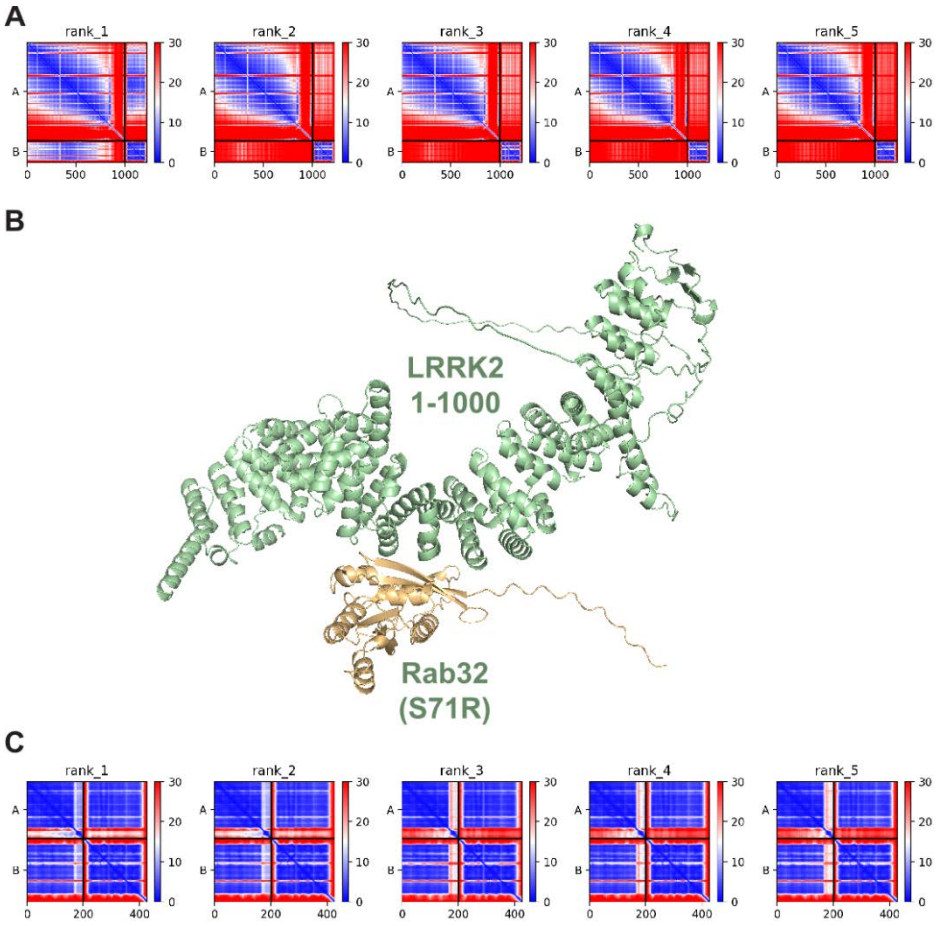

Supplementary Figure 4. A) Predicted aligned error (PAE) plots of 5 models for the LRRK2(1-1000)/RAB32 prediction. **B)** Structure overview of the top model for the LRRK2(1-1000aa)/Rab32 prediction. **C)** PAE plots of 5 models for the LRRK2(350-550aa)/RAB32 prediction**.**

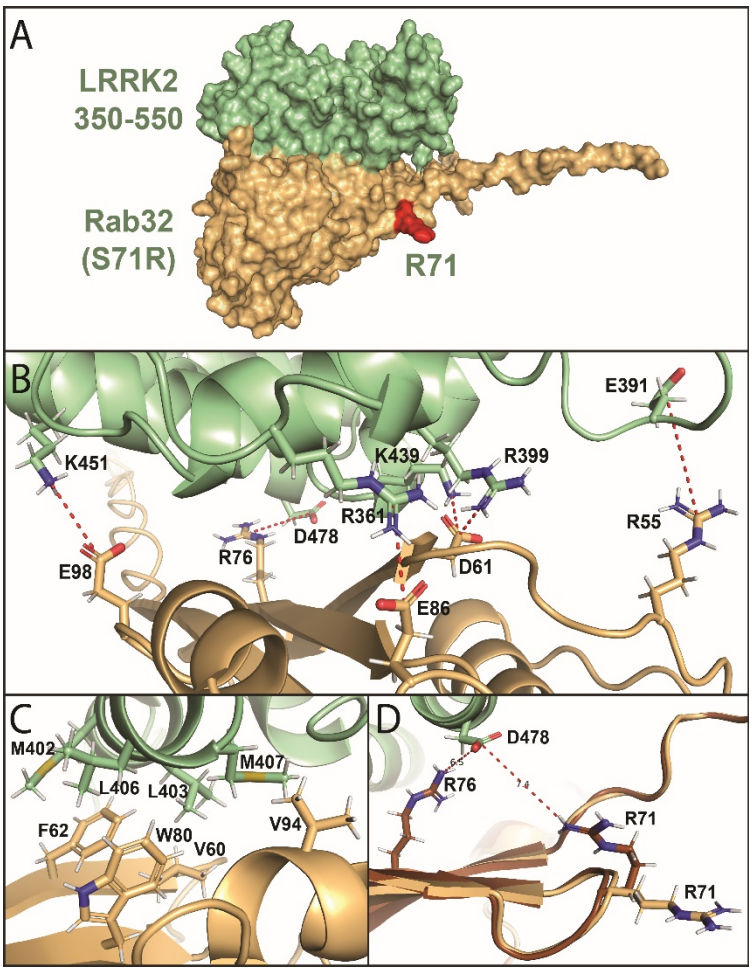

Supplemental Figure 5. Overview of the AlphaFold model of Rab32 (Ser71Arg) and LRRK2(350-550) protein complex (Rab32 Arg71 marked in red) **(A)**, with detailed view of electrostatic **(B)** and hydrophobic **(C)** interactions predicted to be crucial for the protein-protein binding. **(D)** Overlay of 2 different rotamers of the Rab32 Arg71 residue, showing the rotamer (in brown) with a possible electrostatic interaction between Arg71 and LRRK2 Asp478. All models showed a binding interface consistent with interfaces identified for RAB29 and RAB38, with a hydrophobic patch formed by Met402, Leu403, Leu406 and Met407 of LRRK2, interacting with Phe62, Val60, Trp80 and Val94 of RAB32 (**B**). Electrostatic interactions (**C**) were predicted to form between the following pairs of residues (LRRK2 – RAB32): Arg399 – Asp61, Lys451 – Glu98 and Asp478 – Arg76, with additional salt bridges predicted between Arg361 – Glu86, Asp392 – Arg55 and Lys439 – Asp61.

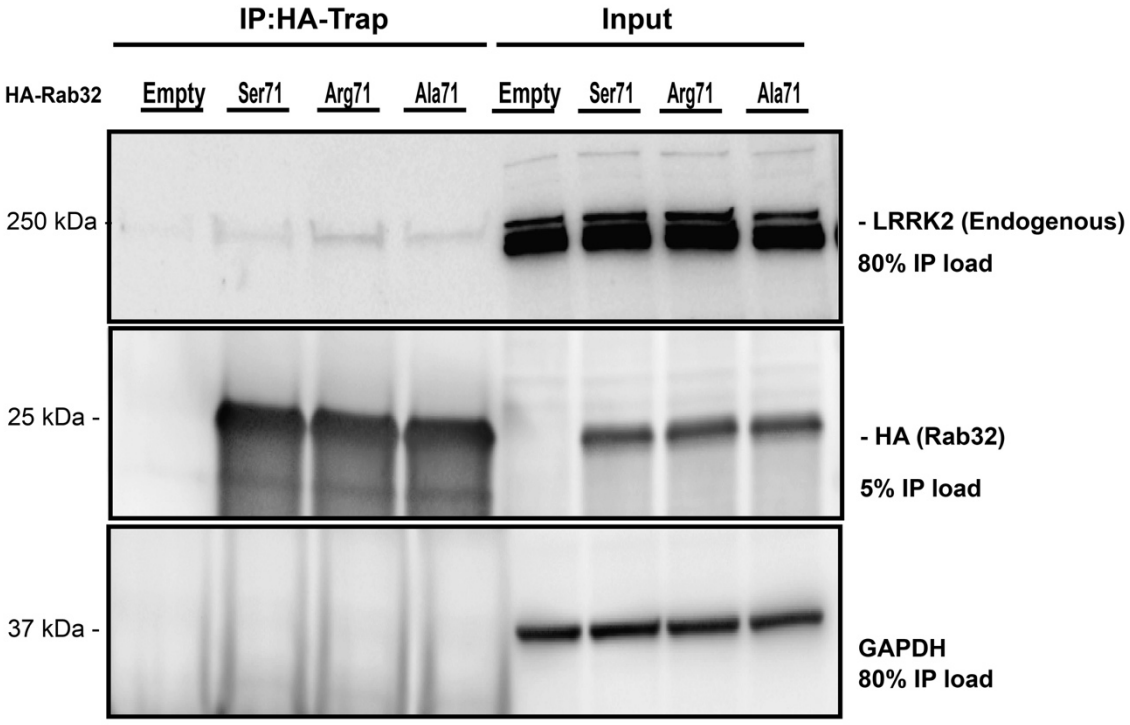

Supplementary Figure 6. HA-RAB32 co-immunoprecipitation of endogenous LRRK2. **A)** Co-Immunoprecipitation analysis of lysates from HEK293FT cells transiently expressing either HA empty vector, HA-RAB32 Ser71 or mutant (Arg71 or Ala71) cDNA. HA-Trap and immunoblot analysis was performed using an anti-HA antibody (middle panel), anti-LRRK2 antibody (top panel) and GAPDH antibody (bottom panel) as indicated. Separate gels from the same IP sample were loaded to limit HA-signal saturation. GAPDH is used for loading and negative control. Input denotes whole cell lysate starting material from HEK293FT cells used for immunoprecipitation analysis.

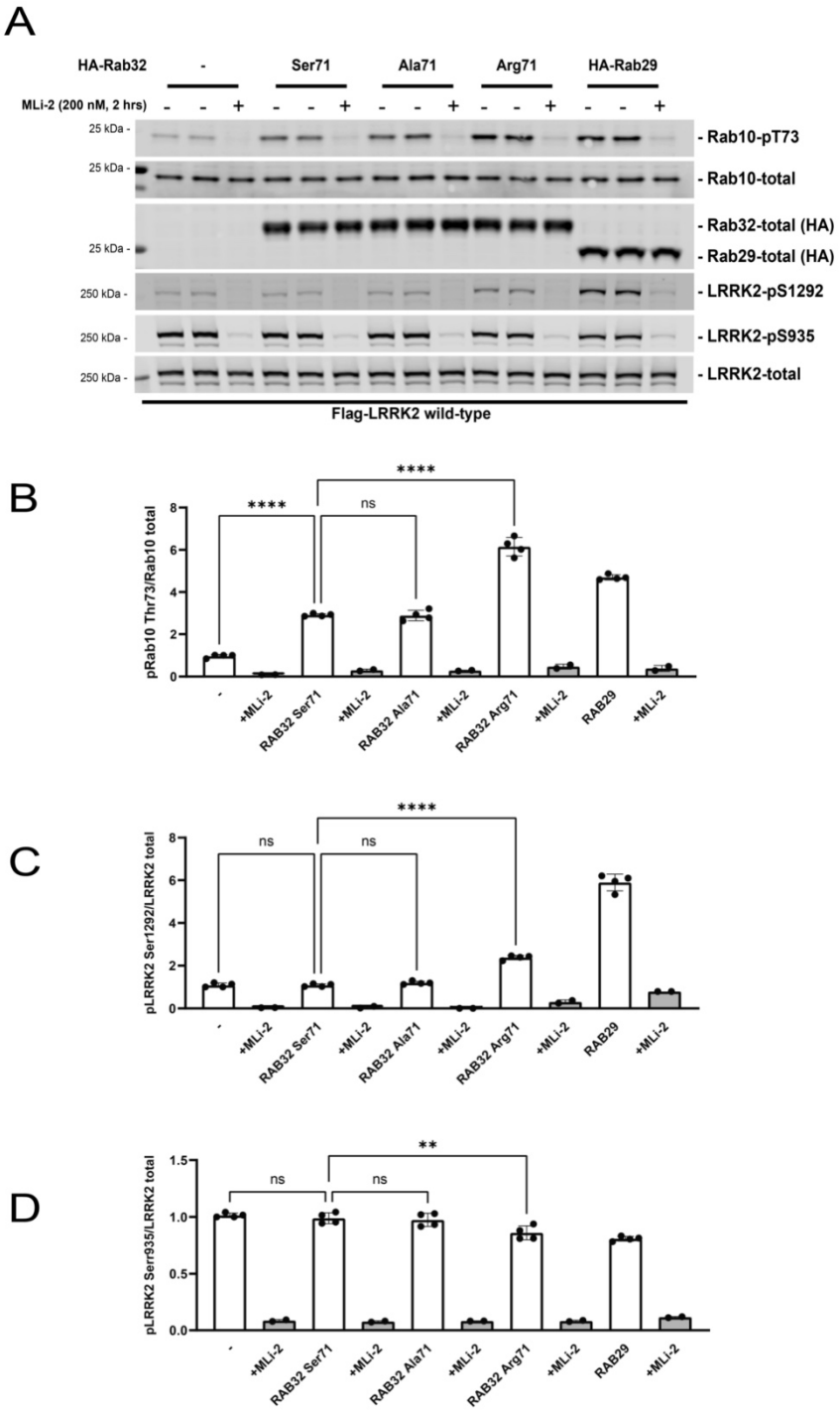

Supplementary Figure 7: Quantitative immunoblotting analysis of the cellular kinase activity of wild-type LRRK2 in the presence of RAB32 (Ser71 wild-type or Arg71 mutant) or Rab29. **A)** HEK293 cells were co-transfected with wild-type LRRK2 and either HA-empty vector (−) or the indicated variants of HA-tagged RAB32 or HA-tagged Rab29, and treated +/- MLi-2 (200 nM, 2 hrs) or DMSO control (0.1% v/v) prior to lysis. **B-D)** Quantitation of phosphorylated RAB10-T73, phosphorylated LRRK2-S1292 and phosphorylated LRRK2-S935 normalized to total RAB10 and total LRRK2 respectively is shown. Error bars indicate mean with SD from two independent experiments, each performed in duplicate. One-way ANOVA tests showed highly significant results for each group of test; pRAB10 $F(4,15) = 27$, $p<0.0001$, LRRK2 pSer1292 $F(4,15)=46$ $p<0.0001$ and LRRK2

pSer935 $F(4,15)=15.6$, $p<0.0001$, and Tukey's multiple comparisons test statistics are illustrated (adjusted $p<0.01$ ** , <0.001***, <0.0001****) and as stated in the main text.

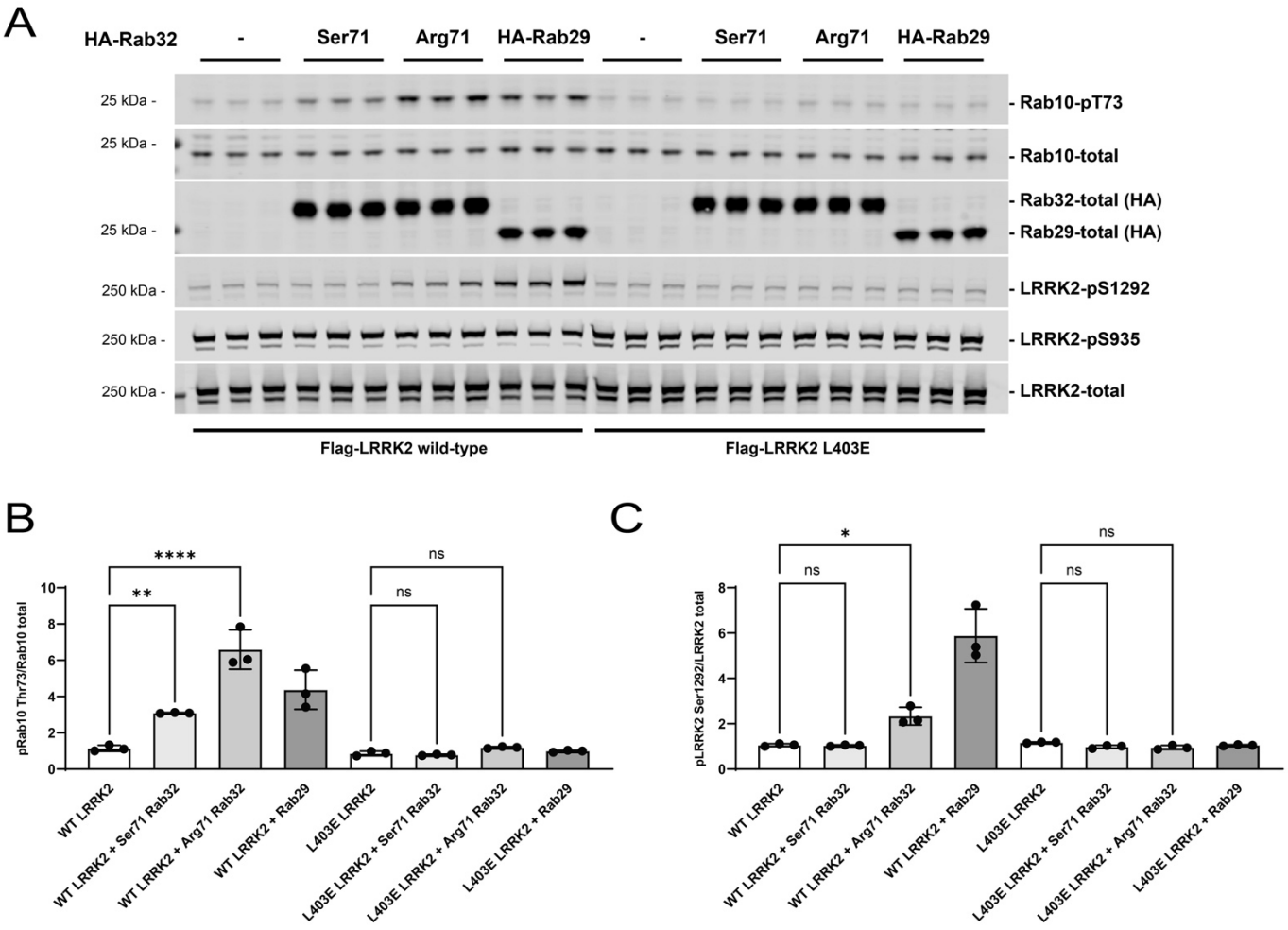

Supplementary Figure 8: Quantitative immunoblotting analysis of the cellular kinase activity of wild-type and LRRK2 Leu403Glu (L403E)[25] in the presence of RAB32 (WT and Ser71 mutant) or RAB29. A) HEK293 cells were co-transfected with either wild-type or LRRK2 L403E and either HA-empty vector (−) or the indicated variants of HA-tagged RAB32 or HA-tagged RAB29, and treated +/- MLi-2 (200 nM, 2 hrs) or DMSO control (0.1% v/v) prior to lysis. B-C) Quantitation of phosphorylated RAB10-T73 and phosphorylated LRRK2-S1292 normalized to total RAB10 and total LRRK2 respectively is shown. Error bars indicate mean with SD from three experiments. Two-way ANOVA tests showed highly significant results for WT and not LRRK2 L403E in each group of tests; pRAB10 $F_{(7,14)}$ =57, p<0.0001, LRRK2 pSer1292 $F_{(7,14)}$ =50 p<0.0001, and Tukey's multiple

comparisons test statistics are illustrated (adjusted p<0.01 ** , <0.001***, <0.0001****) and as stated in the main text.

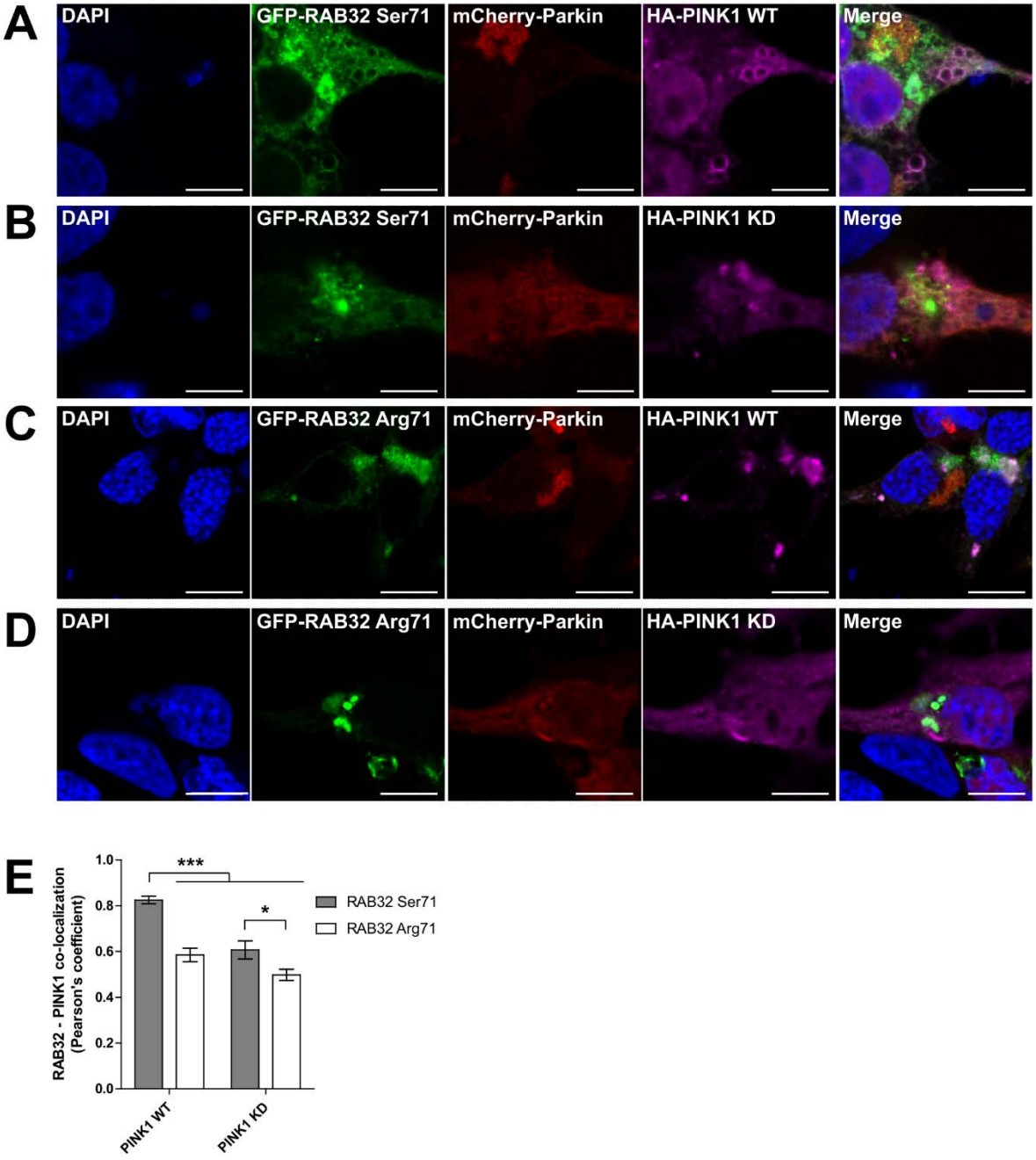

Supplementary Figure 9. RAB32 co-localization with PINK1. Confocal images of HEK293 cells co-transfected with mCherry-Parkin and GFP-tagged wild-type RAB32 **(A, B)** or RAB32 Ser71Arg **(C, D)** and HA-tagged wild-type PINK1 **(A, C)** or kinase dead PINK1 **(B, D)**. Boxes indicate regions shown at higher power below. Scale bars are 10 microns. **(E)** Pearson's correlation coefficient to quantify the co-localization of GFP-RAB32 and HA-PINK1. Bars show mean +/-SEM of 12-15 fields. * indicates $P<0.05$, *** indicates $P<0.0001$ according to ANOVA followed by Tukey's multiple comparison tests.

SUPPLEMENTARY REFERENCES

1 Rajput AH, Rajput A. Saskatchewan Movement Disorders Program. *Canadian Journal of Neurological Sciences* 2015; **42**: 74–87.

2 Wang K, Li M, Hakonarson H. ANNOVAR: functional annotation of genetic variants from high-throughput sequencing data. *Nucleic Acids Res* 2010; **38**: e164–e164.

3 Kircher M, Witten DM, Jain P, O'roak BJ, Cooper GM, Shendure J. A general framework for estimating the relative pathogenicity of human genetic variants. *Nature Genetics 2014 46:3* 2014; **46**: 310–5.

4 Ross OA, Soto-Ortolaza AI, Heckman MG, *et al.* Association of LRRK2 exonic variants with susceptibility to Parkinson's disease: a case–control study. *Lancet Neurol* 2011; **10**: 898–908.

5 Vilariño-Güell C, Wider C, Ross OA, *et al.* VPS35 Mutations in Parkinson Disease. *The American Journal of Human Genetics* 2011; **89**: 162–7.

6 Lorenzo-Betancor O, Ogaki K, Soto-Ortolaza AI, *et al.* DNAJC13 p.Asn855Ser mutation screening in Parkinson's disease and pathologically confirmed Lewy body disease patients. *Eur J Neurol* 2015; **22**: 1323–5.

7 Vilariño-Güell C, Rajput AHAAHAH, Milnerwood AJAJ, *et al.* DNAJC13 mutations in Parkinson disease. *Hum Mol Genet* 2014; **23**: 1794–801.

8 Sidransky E, Nalls MA, Aasly JO, *et al.* Multicenter Analysis of Glucocerebrosidase Mutations in Parkinson's Disease. *New England Journal of Medicine* 2009; **361**: 1651–61.

9 Vilariño-Güell C, Wider C, Soto-Ortolaza AI, *et al.* Characterization of DCTN1 genetic variability in neurodegeneration. *Neurology* 2009; **72**: 2024–8.

10 Zimprich A, Biskup S, Leitner P, *et al.* Mutations in LRRK2 cause autosomal-dominant parkinsonism with pleomorphic pathology. *Neuron* 2004; **44**: 601–7.

11 Furtado S, Payami H, Lockhart PJ, *et al.* Profile of families with parkinsonism-predominant spinocerebellar ataxia type 2 (SCA2). *Mov Disord* 2004; **19**: 622–9.

12 West A, Periquet M, Lincoln S, *et al.* Complex relationship between Parkin mutations and Parkinson disease. *Am J Med Genet* 2002; **114**: 584–91.

13 Trinh J, Gustavsson EK, Vilariño-Güell C, *et al.* DNM3 and genetic modifiers of age of onset in LRRK2 Gly2019Ser parkinsonism: a genome-wide linkage and association study. *Lancet Neurol* 2016; **15**: 1248–56.

14 Gustavsson EK, Trinh J, McKenzie M, *et al.* Genetic Identification in Early Onset Parkinsonism among Norwegian Patients. *Mov Disord Clin Pract* 2017; **4**: 499–508.

15 Jumper J, Evans R, Pritzel A, *et al.* Highly accurate protein structure prediction with AlphaFold. *Nature* 2021; **596**: 583–9.

16 Mirdita M, Schütze K, Moriwaki Y, Heo L, Ovchinnikov S, Steinegger M. ColabFold: making protein folding accessible to all. *Nat Methods* 2022; **19**: 679–82.

17 Collado-Torres L, Nellore A, Kammers K, *et al.* Reproducible RNA-seq analysis using recount2. Nat Biotechnol. 2017. DOI:10.1038/nbt.3838.

18 Cataldi S, Follett J, Fox JD, *et al.* Altered dopamine release and monoamine transporters in Vps35 p.D620N knock-in mice. *npj Parkinson's Disease 2018 4:1* 2018; **4**: 1–11.

19 Assessment of in vitro kinase activity of over-expressed and endogenous LRRK2 immunoprecipitated from cells. https://www.protocols.io/view/assessment-of-in-vitro-kinase-activity-of-over-exp-4r3l24r63g1y/v1 (accessed Jan 28, 2024).

20 Steger M, Tonelli F, Ito G, *et al.* Phosphoproteomics reveals that Parkinson's disease kinase LRRK2 regulates a subset of Rab GTPases. *Elife* 2016; **5**. DOI:10.7554/eLife.12813.

21 Mir R, Tonelli F, Lis P, *et al.* The Parkinson's disease VPS35[D620N] mutation enhances LRRK2-mediated Rab protein phosphorylation in mouse and human. *Biochemical Journal* 2018; **475**: 1861–83.

22 Zhu H, Tonelli F, Alessi DR, Sun J. Structural basis of human LRRK2 membrane recruitment and activation. *bioRxiv* 2022; : 2022.04.26.489605.

23 Koyano F, Okatsu K, Kosako H, *et al.* Ubiquitin is phosphorylated by PINK1 to activate parkin. *Nature 2014 510:7503* 2014; **510**: 162–6.

24 Lai Y, Kondapalli C, Lehneck R, *et al.* Phosphoproteomic screening identifies Rab GTP ases as novel downstream targets of PINK 1 . *EMBO J* 2015; **34**: 2840–61.

25 Zhu H, Tonelli F, Turk M, Prescott A, Alessi DR, Sun J. Rab29-dependent asymmetrical activation of leucine-rich repeat kinase 2. *Science (1979)* 2023; **382**: 1404–11.